



Deposition of diesel exhaust particles in the human lungs: theoretical simulations and experimental data

Robert Sturm

Division of Physics and Biophysics, Department of Chemistry and Physics of Materials, University of Salzburg, Salzburg, Austria

Correspondence to: Dr. Robert Sturm. Division of Physics and Biophysics, Department of Chemistry and Physics of Materials, University of Salzburg, Hellbrunner Str. 34, Salzburg A-5020, Austria. Email: sturm_rob@hotmail.com.

Background: Based on numerous experimental and epidemiological studies diesel exhaust particles (DEPs) have been evaluated as serious health hazards, whose uptake by inhalation causes an increase of the relative risk for lung cancer. Due to this circumstance, experimental and theoretical knowledge on the transport and deposition behaviour of such particles in the respiratory tract has to be permanently improved. Here, respective support is provided by models predicting aggregate shape and transport with high accuracy.

Methods: Aggregate shape was modeled by using the computer program AGGREGATE, where respective particles are constructed from equally sized spherules by application of the random walk concept. Intrapulmonary transport and deposition of the particulate mass were simulated for a stochastic lung architecture and under the assumption of mathematically describable deposition mechanisms (Brownian motion, inertial impaction, interception, gravitational settling). Computations were conducted for particles ranging in size from 50 to 250 nm. In addition, three different breathing scenarios (sitting, light exercise, heavy exercise) were considered.

Results: According to the results of the deposition computations theoretically constructed DEP aggregates exhibit decreasing total and regional deposition with growing particle diameter. Depending on aggregate size and breathing conditions, total deposition ranges from 15.7% to 71.5%, whereas tubular deposition adopts values between 10.1% and 35.2%. Alveolar deposition may be quantified with 4.7% to 27.0%. Except for alveolar accumulation of aggregates ≤ 100 nm, deposition of DEPs negatively correlates with breathing intensity. Local deposition of such aggregates is commonly characterized by the development of respective modes in airway generations 20 to 22.

Conclusions: The present study leads to the conclusion that DEPs may bear the potential for an increased deposition in those lung regions, which are highly susceptible for the development of lung cancer. Thereby, the amount of particulate mass accumulated in airways and alveoli depends on both particle size and the intensity of particle uptake by inhalation.

Keywords: Diesel exhaust particle (DEP); aggregate; random walk model; deposition; respiratory tract; Brownian motion

Received: 17 May 2017; Accepted: 06 June 2017; Published: 25 July 2017.

doi: 10.21037/jphe.2017.06.07

View this article at: <http://dx.doi.org/10.21037/jphe.2017.06.07>

Introduction

In general, diesel exhaust has to be regarded as complex mixture of combustion products of diesel fuel. The exact composition of this mixture, however, depends on numerous factors, among which the type of engine, operating conditions, the oil used for lubrication, additives, presence of an emission control system, and fuel composition play an essential role (1,2). According to several studies conducted in the 1980s diesel engines of light-duty vehicles (automobiles, light trucks) emit 50 to 80 times as much particulate mass as typical catalyst-equipped gasoline engines, whereas diesel engines of heavy-duty vehicles (trucks) even produce a particle emission, which is 100 to 200 times as high as that of gasoline cars (3). Experimental investigations could furnish proof that the vast majority of diesel exhaust particles (DEPs) is characterized by aerodynamic diameters ranging from 0.10 to 0.25 μm (4-7). Furthermore, it could be demonstrated that the particle size distribution of diesel exhaust has to be evaluated as bimodal, with a strict separation between particles formed by nucleation and those generated by agglomeration of nuclei particles (8,9). With regard to its chemical composition diesel exhaust shows some specific features: Besides an inorganic fraction primarily consisting of small elemental carbon particles (0.01 to 0.08 μm), it contains organic compounds, sulfate, and some inorganic additives and components of fuel and motor oil (10). The organic compounds included in diesel exhaust emissions among other consist of hydrocarbons, hydrocarbon derivatives, aldehydes, polyaromatic hydrocarbons (PAHs), PAH derivatives, multifunctional PAH derivatives, heterocyclic compounds, heterocyclic derivatives, and multifunctional derivatives of heterocyclic compounds (11).

DEPs are marked by their large surface area, which facilitates the adsorption of large amounts of organic material originating from unburned fuel, lubricating oil, and pyrosynthesis during fuel combustion. Among these organic substances several compounds, such as PAHs and nitro-PAHs, have to be classified as mutagens and carcinogens (12,13). Concerning the carcinogenicity of diesel exhaust, most data supporting such hazardous effects come from experiments with laboratory animals (14-16) and mechanistic studies (15-19). Scientific investigations conducted in humans, on the other side, have only yielded limited evidence for the noxious potential of DEPs hitherto. In the majority of contributions occupational exposure to the exhaust of diesel engines was directly associated with

enhanced rates of lung cancer, whereby transportation and construction workers crystallized out as highly neuralgic group of probands (17,20,21). Since the identification of DEPs as human carcinogens (17-21) numerous additional epidemiological studies have been carried out. They unanimously came to the conclusion that exposure to diesel exhaust increases the relative risk for lung cancer by a factor of 1.2 to 2.21 (22-30). Any adjustments for smoking or other exposures did not significantly alter this enhancement in risk. In addition, it could be found that also other tissue sites, particularly the urinary bladder, bear increased risks of cancer (31,32).

Experimental studies focusing on the aerodynamics of DEP in the various structures of the respiratory tract can be subdivided into two categories: besides investigations of particle behaviour in artificial casts of parts of the tracheobronchial tree (33) also respective research including inhalation uptake of particulate mass by human probands can be recognized (34-36). Concerning the theoretical simulation of DEP deposition in the human respiratory tract a continuous increase of predictive accuracy could be achieved during the past decade (37-44). This circumstance may be, among other, related to a more precise modeling of irregular particle shapes (45,46) and the application of stochastic lung architectures (47-52), which allow the generation of almost realistic frame conditions. According to the results presented in the experimental and hypothetical studies DEPs preferably deposit in the upper and central airways of the respiratory tract under normal breathing conditions. Any increase of the inhalation flow rate, however, results in the enhanced transfer of the particulates into the alveolar region combined with their intensified deposition in the lung bubbles.

The present contribution pursues two main goals: Firstly, a comprehensive theoretical description of DEP deposition in the human lung is provided, thereby using new findings of particle generation, which are included in the computer program AGGREGATE (53) developed by the author. Secondly, the predictive power of the model is subjected to a thorough validation process, where available experimental data are compared with related hypothetical results. The work presents several innovative aspects:

- ❖ Precise generation of almost realistic particle shapes is combined with a highly validated particle transport and deposition model as well as a stochastic lung architecture.
- ❖ Deposition computations are based on findings of both empirical and numerical studies and thus bear

enhanced accuracy.

- ❖ The particle generation software enables the rapid construction of a high variety of particulate shapes occurring in the ambient air and therefore represents a reliable approach to the natural conditions.

Methods

Theoretical generation of DEP aggregates

According to microscopic studies DEPs form aggregates of irregular shape, which typically consist of equally sized spherical components (*Figure 1*). The aggregates are often characterized by rather equal extension along the three axes of a spatial coordinate system (isometric cluster), but can also occur as chain-like or disk-like constructs. In the first case, single components are preferably arranged along one coordinate axis, whereas extension of the aggregate along the remaining spatial directions is significantly reduced ($x \gg y \sim z$). In the second case, main extension of the aggregates takes place along two coordinate axes, whilst the third spatial dimension remains remarkably underrepresented ($x \sim y \gg z$).

The theoretical approach to the irregular aggregate structure of DEPs was conducted by using the computer code AGGREGATE that had been recently introduced by the author (53). The program is founded upon a random walk algorithm, according to which arrangement of single spherical components along the three coordinate axes takes place with the help of a random number concept. Starting from the origin of the coordinate system single components may be added along six directions of the spatial coordinate system (+x, -x, +y, -y, +z, -z; *Figure 1B-D*). After occupation of a certain position, the next one is simulated by the program, until the number of pre-defined components is reached. If a position is already occupied by a spherule, an additional random walk step is included in the particle generation routine.

For particulate aggregates constructed in the way described in *Figure 1B-D* most essential aerodynamic parameters such as dynamic shape factors and particle-related diameters were computed immediately after definition of the geometric models (*Figure 2*). Dynamic shape factors of isometric clusters were approximated by using the simple equations of Kasper (54), whereas respective factors of anisometric aggregate structures were obtained from more complex approaches described by the same author as well as by Sturm (55). In general,

isometric clusters are marked by dynamic shape factors ≥ 1 , whereby internal voids cause a continuous increase of this aerodynamic quantity. In the case of anisometric aggregates irregular structures are typically approximated by using well defined geometric shapes such as elongated cylinders, round platelets or prolate and oblate spheroids (51-55). Dynamic shape factors of these geometric substitutes are usually greater or even much greater than 1 and depend on the so-called aspect ratio (= length/width) of the particle (55-57). For elongated particles any increase of the aspect ratio results in an enhancement of the dynamic shape factors, whilst for flat platelets a similar effect can be observed by permanently reducing the aspect ratio. As depicted in *Figure 2*, highly anisometric aggregates and their related geometric substitutes are characterized by two distinct dynamic shape factors, one of them being valid for particle orientation parallel to the stream lines of the inhaled air, the other for particle orientation perpendicular to the stream lines. Concerning aggregates ranging in size from 10 to 250 nm random particle orientation was assumed throughout the whole respiratory tract, thereby using a mean value of the two dynamic shape factors noted above and described in *Figure 2* (55-57).

Particle deposition modeling outlined in the next section was commonly conducted after determination of aerodynamic particle diameters. As demonstrated in the graph of *Figure 3*, the aerodynamic diameter typically increases with the number of spherical components included in the particulate aggregate. Whilst for isometric clusters this physical quantity develops from 100 (1 component à la 100 nm) to 458 nm (1,000 components à la 100 nm), for chain-like aggregates an increase of the aerodynamic diameter from 100 to 478 nm may be observed. With regard to disk-like aggregates a respective development of the aerodynamic diameter from 100 to 517 nm may be recognized.

Deposition of DEP aggregates—modeling assumptions

Deposition of inhaled DEPs in the respiratory tract was simulated by assuming: (A) a stochastic architecture of the tracheobronchial tree; (B) randomly selected particle trajectories through the bronchial and bronchiolar airway sequences; and (C) a deposition of intrapulmonary transported aggregates according to mathematically approachable mechanisms (Brownian motion, inertial impaction, interception, gravitational settling) (45-55). For the theoretical generation of statistically reliable particle

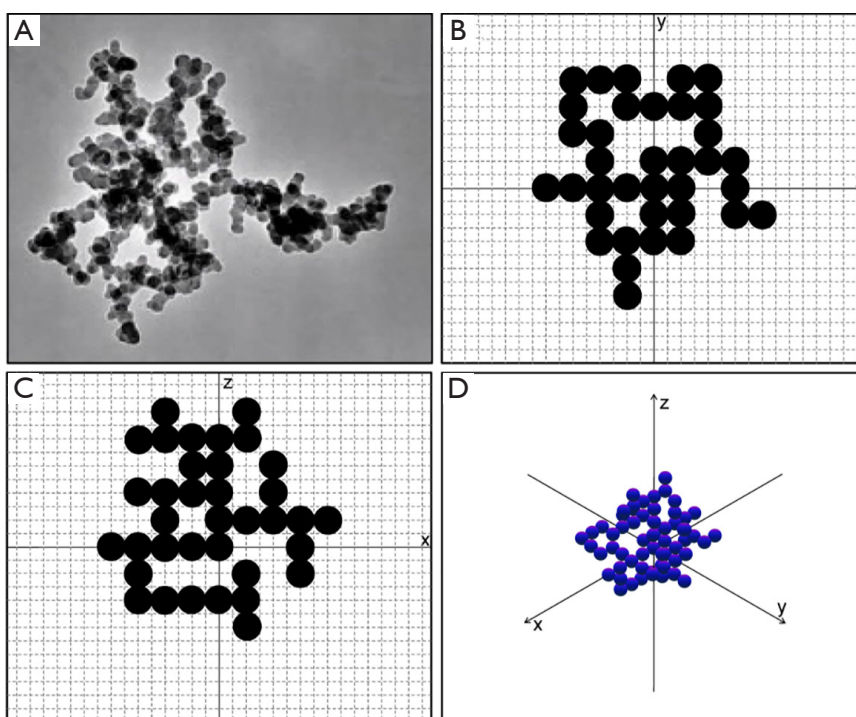


Figure 1 Random walk model for the simulation of DEP shape: (A) microscopic appearance of a typical aggregate originating from the combustion of diesel fuel; (B) projection of a modeled aggregate on the X-Y plane; (C) projection of a modeled aggregate on the X-Z plane; (D) spatial appearance of the theoretical DEP simulated with the program AGGREGATE (53). DEP, diesel exhaust particle.

transport and deposition scenarios the Monte Carlo technique (calculation of a high number of particle paths) as well as the method of statistical weights allowing multiple deposition events for a given particle were applied (45,46). Results produced by the deposition program were presented in different ways: Besides illustrating the effect of particle size (expressed in terms of the aerodynamic diameter) on total and regional (i.e., tubular and alveolar) deposition, also the dependence of local (i.e., generation-specific) deposition on particulate dimension was demonstrated for selected DEP aggregates (50, 150, 250 nm). The density of the generated aggregates was uniformly set to $1 \text{ g}\cdot\text{cm}^{-3}$ (unit-density).

Aggregate deposition computations were conducted under the assumption of three different breathing scenarios (58): sitting breathing includes particle uptake through the nasal airways, a tidal volume of 750 cm^3 , and a breath-cycle time of 5 s (breath-hold: 1 s). Light-exercise breathing, on the other hand, is distinguished by oral inhalation, a tidal volume of $1,250 \text{ cm}^3$, and a breath-cycle time of 3 s (no breath-hold). Heavy-exercise breathing, finally, is characterized by oral inspiration, a tidal volume

of $1,900 \text{ cm}^3$, and a breath-cycle time of 2 s (no breath-hold). Computations were carried out for an average lung of a male Caucasian adult (functional residual capacity: $3,300 \text{ cm}^3$), thereby supposing an additional extrathoracic volume of 50 cm^3 .

Results

Total and regional lung deposition of variably sized aggregates

Under sitting breathing conditions total, tubular, and alveolar deposition of diesel aggregates are subject to a continuous decline with particle size increasing from 50 to 250 nm (Figure 4A). Whilst total deposition on average decreases from 71.5% to 25.3%, particle accumulation in the tubular structures exhibits an average reduction from 35.2% to 13.6% and deposition in the alveoli develops from 22.7% to 5.3%. A switch from sitting breathing to light-exercise breathing has several consequences for the deposition of diesel aggregates in the human respiratory tract. Total deposition of the particulates generally becomes

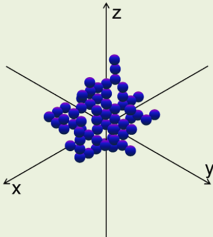
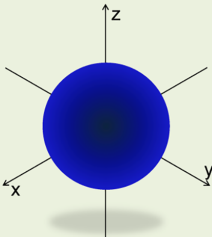
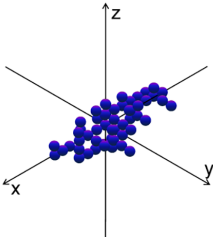
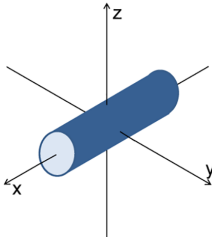
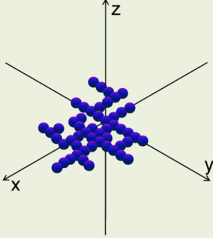
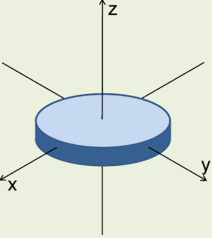
Aggregate shape	Approximated geometry	Dynamic shape factor	References
 <p>Isometric cluster ($x \sim y \sim z$)</p>	 <p>Sphere</p>	$\chi = d_{es}/d_{ev}$ $d_{ev} = n^{1/3} \cdot d_c$ <p>d_{es} ... Diameter of enveloping sphere d_{ev} ... Diameter of volume-equivalent sphere d_c ... Diameter of spherical component n ... Number of spherical components</p>	Kasper, 1982 [54]
 <p>Chain-like cluster ($x \gg y \sim z$)</p>	 <p>Cylinder</p>	$\chi_{\perp} = \frac{\frac{8}{3}(\beta^2 - 1)\beta^{-1/3}}{2\beta^2 - 3 - \frac{\ln(\beta + \sqrt{\beta^2 - 1})}{\sqrt{\beta^2 - 1}} + \beta}$ $\chi_{\parallel} = \frac{\frac{4}{3}(\beta^2 - 1)\beta^{-1/3}}{2\beta^2 - 1 - \frac{\ln(\beta + \sqrt{\beta^2 - 1})}{\sqrt{\beta^2 - 1}} - \beta}$ <p>χ_{\perp} ... Dynamic shape factor, perpendicular particle orientation χ_{\parallel} ... Dynamic shape factor, parallel particle orientation β ... Particle aspect ratio (length/width)</p>	Kasper, 1982 [54] Sturm, 2010 [55]
 <p>Disk-like cluster ($x \sim y \gg z$)</p>	 <p>Round platelet</p>	$\chi_{\perp} = \frac{\frac{8}{3}(\beta^2 - 1)\beta^{-1/3}}{2\beta^2 - 3 - \arccos \beta + \beta}$ $\chi_{\parallel} = \frac{\frac{4}{3}(\beta^2 - 1)\beta^{-1/3}}{2\beta^2 - 1 - \arccos \beta - \beta}$ <p>χ_{\perp} ... Dynamic shape factor, perpendicular particle orientation χ_{\parallel} ... Dynamic shape factor, parallel particle orientation β ... Particle aspect ratio (length/width)</p>	Kasper, 1982 [54] Sturm, 2010 [55]

Figure 2 DEP aggregate shapes, their approximations with regular geometric bodies, and their related dynamic shape factors. DEP, diesel exhaust particle.

reduced by several percent and decreases from 62.6% to 18.9%, when particle size is increased from 50 to 250 nm. A similar but noticeably weakened trend can be recognized for tubular deposition, which declines from 33.5% to 12.6% within the given particle size range. Alveolar deposition becomes enhanced for particle sizes ≤ 100 nm but decreased for sizes >100 nm. In general, particle accumulation in the lung bubbles develops from 26.5% to 5.2% (Figure 4B). Under heavy-exercise breathing conditions those tendencies observed after the change from sitting to light-work inhalation are further continued and intensified. Concretely speaking, average total deposition is characterized by a decrease from 55.7% to 15.7%, whereas tubular particle deposition develops from 26.6% to 10.1% and alveolar deposition from 27.0% to 4.7% (Figure 4C).

Generation-specific deposition of aggregates with different sizes

According to the model predictions DEPs are generally marked by the tendency of an increased deposition in central and distal airways (generations 10–25, Figure 5). The proximal airways (generations 1–10), on the other hand, are uniformly distinguished by relative deposition values $<1.00\%$. Under sitting breathing conditions maximal deposition of 50-nm aggregates occurs in generation 21 and adopts an average value of 7.06%. With regard to aggregates measuring 150 and 250 nm in size, highest deposition could be predicted for generation 20, thereby assuming average values of 3.46% and 2.23%, respectively (Figure 5A). Transition from sitting to light-exercise breathing commonly results in a slight reduction

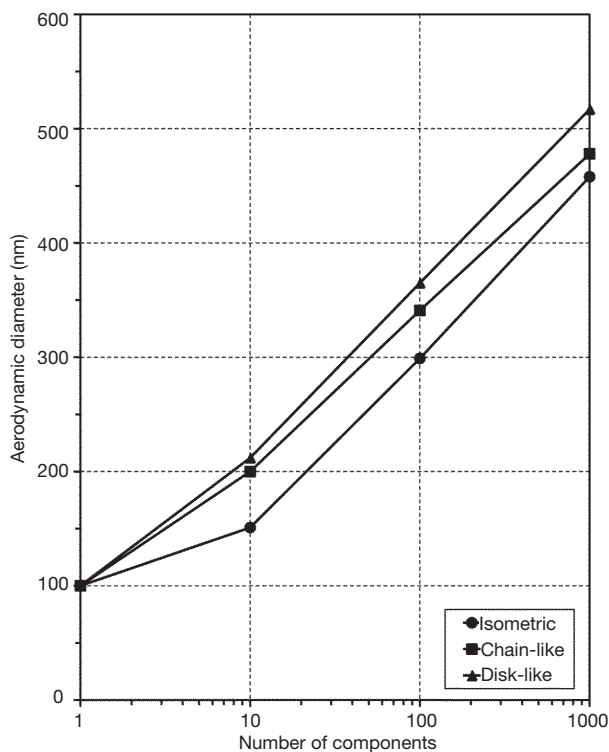


Figure 3 Dependence of the aerodynamic diameter of modeled DEP on the number of spherical components (size of one component: 100 nm; see *Figure 1*) and the basic type of approximated geometric shape. DEP, diesel exhaust particle.

of average generation-specific deposition values. Highest deposition of 50-nm aggregates, which is again located in generation 21, amounts to 6.99%, whereas maximal deposition values of 150 and 250 nm aggregates (both also predicted for generation 21) have to be figured out at 3.09% and 2.21% (*Figure 5B*). Heavy-work breathing causes a further reduction of generation-related deposition of DEP aggregates and, as a side effect, the displacement of the modes towards more distal lung regions. In concrete terms, maximal values are now predicted for generation 22 and amount to 6.73%, 2.51%, and 1.80%, respectively (*Figure 5C*).

Validation of the aggregate generation and deposition model

For an appropriate quality management, the used mathematical approach was validated with experimental data of DEP deposition in the human lungs (34-36). All physical and physiological frame conditions outlined in

these studies were included in the model input routines and subjected to comprehensive computations. Results of the experimental lines and related theoretical simulations were plotted in an X-Y-diagram in order to optimize comparison of the data sets (*Figure 6*). As demonstrated in the respective graph differences of the data sets vary between 0 and 10% and are therefore rather moderate. All three experimental data sets could be simulated with almost identical accuracy, which generally underlines the predictive quality of the model.

Discussion

In the present contribution, a mathematical approach for the generation of particle aggregates ranging in size from 50 to 250 nm was subject to a detailed description. In addition, aerodynamic behaviour of such particulate constructs in the human respiratory tract was modeled for different breathing scenarios. Based on predictions produced with the mathematical model three central statements can be made: (A) total and regional deposition exhibit a valuable decline with increasing particle size; (B) any enhancement of the tidal volume and the related inhalation flow rate results in a diminution of total and tubular deposition. In the case of aggregate deposition in the alveolar structures things become a little more complicated insofar as small DEPs (≤ 100 nm) are subject to increased deposition, whereas larger DEPs (> 100 nm) also deposit with lower quantities; (C) with regard to local deposition inhaled DEP aggregates belonging to three size categories (50, 150, 250 nm) produce deposition modes in peripheral airway generations (No. 20–22). Any intensification of breathing causes a slight mode-shift in distal direction.

With regard to the first point raised above it has to be noted that particulates of the nano-scale (≤ 100 nm) are highly affected by the surrounding gaseous medium. Due to a continuous collisional interaction between particles and gas molecules enhanced diffusive transport in radial direction and related deposition can be recognized (46-53). Particulates exceeding the nano-scale (> 100 nm), on the other side, have to be attributed to a transition flow regime, where they prove to be too large for intense diffusion-based transport, but still too small for an enhanced effect of mass-related transport mechanisms (inertial impaction, interception, gravitational settling) (56,57). As main result of this physical phenomenon intrapulmonary particle deposition permanently declines within a particle size interval ranging from 50 to 250 nm. In this context, it has

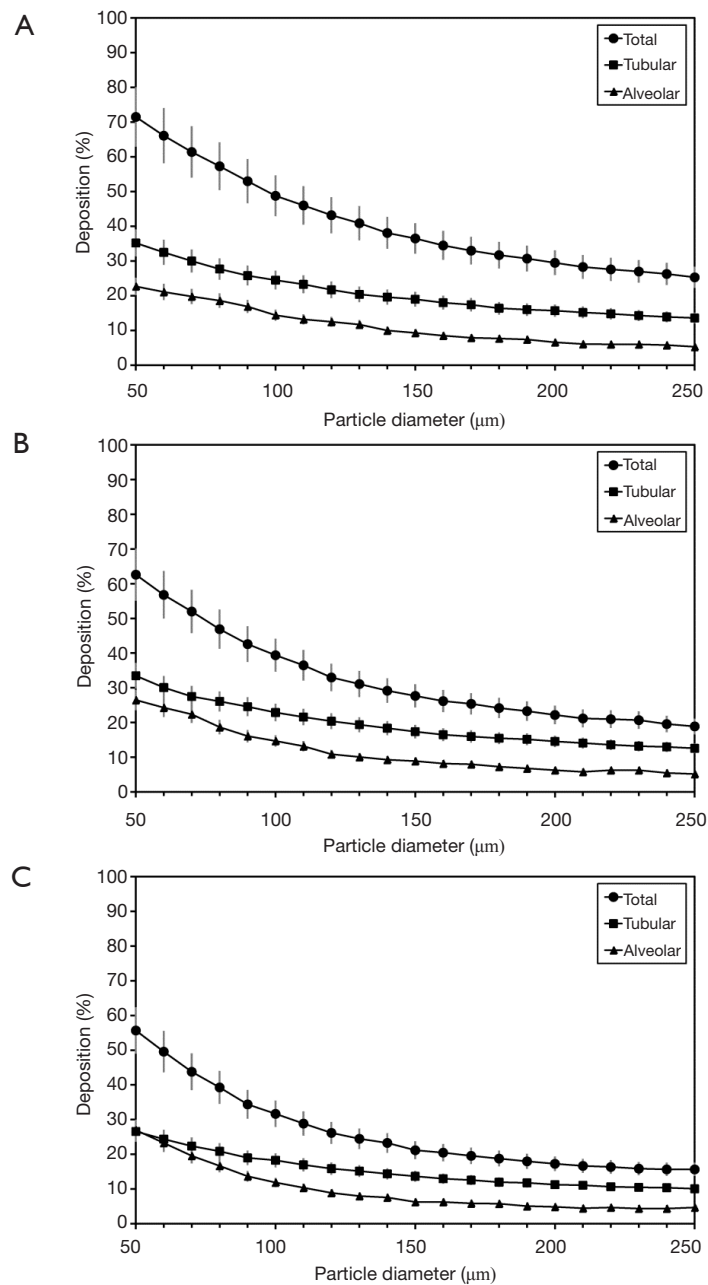


Figure 4 Dependence of total and regional (= tubular and alveolar) DEP deposition on the size of inhaled aggregates (mean \pm standard deviation): (A) sitting breathing; (B) light-exercise breathing; (C) heavy-exercise breathing. DEP, diesel exhaust particle.

to be added that extremely small particles (<10 nm) and large particles (>1 μm) are most significantly influenced by diffusion and mass-related transport mechanisms, respectively, which results in the generation of highest deposition intensities (46-53).

Predicted reduction of DEP aggregate deposition with

increasing inhalation flow rate originates from the fact that axial transport velocity of the inspired particulate mass is raised remarkably and the time span allocated for radial diffusion is simultaneously reduced (50-52). Consequences emerging from this predominance of axial transport over radial diffusion include the relocation of maximal particle

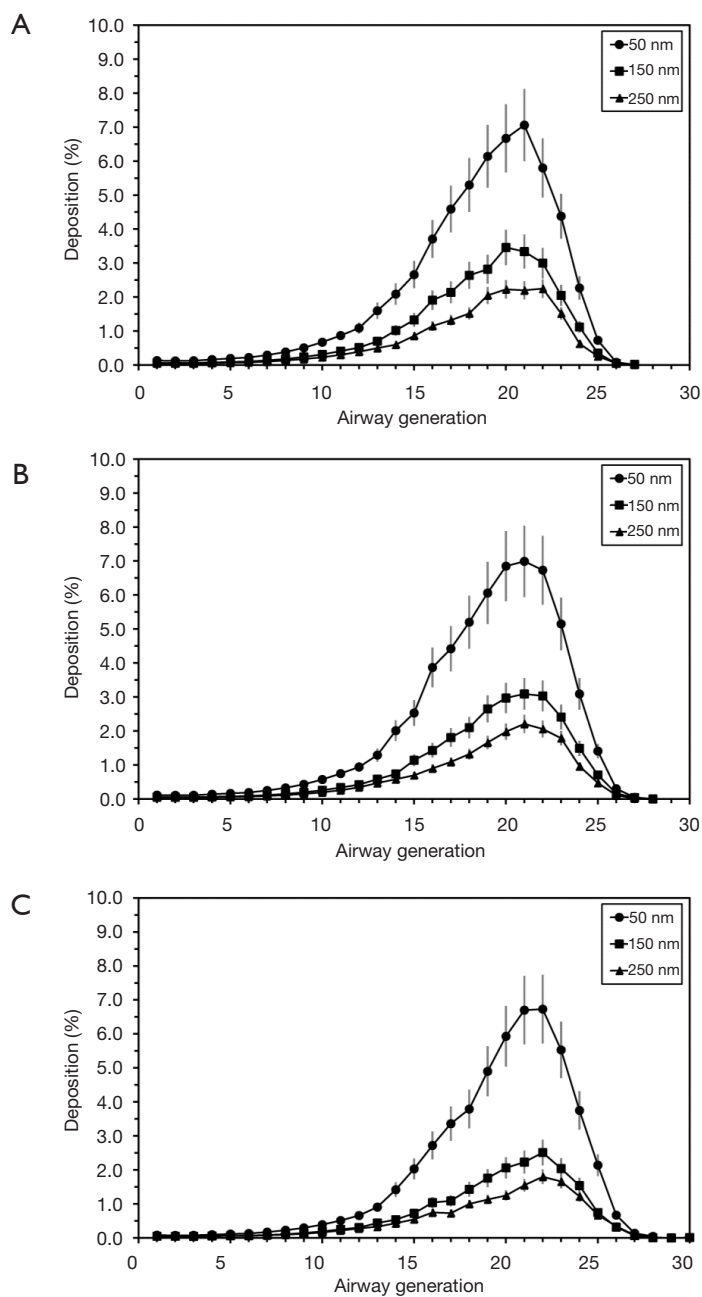


Figure 5 Local deposition (mean \pm standard deviation) of variably sized DEP in airway generations 1 (= trachea) to 30 (= respiratory bronchioles): (A) sitting breathing; (B) light-exercise breathing; (C) heavy-exercise breathing. DEP, diesel exhaust particle.

deposition into the deeper lung and the noticeable increase of the exhaled particle fraction (46-53,58). The reasons for central to peripheral airway generations (No. 15-25) occurring as primary targets, on the one hand, include the described competition between axial and radial particle transport. On the other hand, the diffusion coefficient,

representing the core quantity of diffusive processes, indirectly correlates with the square of the particulate diameter (56,57). Therefore, a fivefold increase of DEP aggregate size from 50 to 250 nm results in a decrease of the diffusion coefficient to one-twenty-fifth and a respective retardation of radial particle transfer. In the small

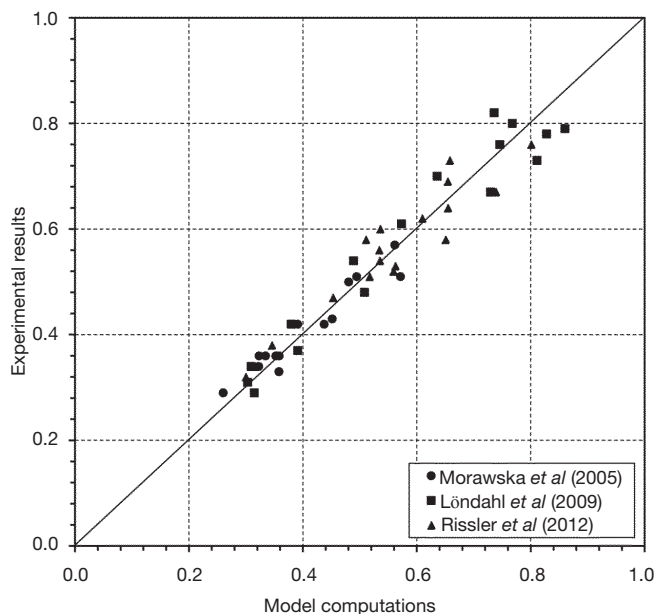


Figure 6 Direct comparison between experimental deposition data of DEP (34-36) and related theoretical predictions, which were conducted by using identical physical and physiological frame conditions. DEP, diesel exhaust particle.

airways, inner tubular diameters are on the order of several millimeters (58), so that aggregates have to surmount shorter diffusive distances and deposition probability is again subject to an increase. Positive correlation of alveolar deposition of aggregates ≤ 100 nm and inhalation flow rate is mainly founded upon the circumstance that with increasing physiological effort larger particle fractions are enabled to enter the lung bubbles, where they have to surmount diffusion distances ranging from 50 to 150 μm (58).

Particulate aggregates deposited in the human respiratory tract are commonly seized by an innate defense system consisting of various clearance scenarios (59-65). Whilst DEPs accumulated in the tracheobronchial airways mainly undergo fast mucociliary or slow bronchial clearance, particulate mass deposited in the alveoli is subject to much slower clearance mechanisms including phagocytotic activity of macrophages and transcytotic transport processes with final accumulation in blood capillaries and lymph vessels. In general, fast particle clearance is completed after about 24 hours, whereas slow bronchial clearance takes place over a time span ranging from 25 to about 100 days. Alveolar clearance, finally, may last several months or, in the case of subepithelial particle storage, even few years (58-65).

Conclusions

From the results presented in this contribution it may be concluded that: (A) DEPs forming variably sized and shaped aggregates mainly undergo diffusive transport processes in the respiratory tract; (B) diffusion-based deposition of these particulate structures chiefly depends on bronchial morphometry and breathing conditions; and (C) central to peripheral airways as well as alveoli occur as main targets of aggregate deposition. Due to the last point, aggregates originating from combustion processes of diesel fuel have to be evaluated as serious health hazards after inhalation uptake.

Acknowledgments

Funding: None.

Footnote

Conflicts of Interest: The author has completed the ICMJE uniform disclosure form (available at <http://dx.doi.org/10.21037/jphe.2017.06.07>). The author has no conflicts of interest to declare.

Ethical Statement: The author is accountable for all aspects of the work in ensuring that questions related to the accuracy or integrity of any part of the work are appropriately investigated and resolved.

Open Access Statement: This is an Open Access article distributed in accordance with the Creative Commons Attribution-NonCommercial-NoDerivs 4.0 International License (CC BY-NC-ND 4.0), which permits the non-commercial replication and distribution of the article with the strict proviso that no changes or edits are made and the original work is properly cited (including links to both the formal publication through the relevant DOI and the license). See: <https://creativecommons.org/licenses/by-nc-nd/4.0/>.

References

1. Obert EF. editor. Internal Combustion Engines and Air Pollution, 3rd ed. New York: Harper and Row, 1973.
2. Ullman TL. Investigation of the Effects of Fuel Composition on Heavy Duty Diesel Engine Emissions. SAE Technical Paper No. 892072. Society of Automotive

- Engineers, 1989.
3. McClellan RO. Toxicological effects of emissions from diesel engines. *Dev Toxicol Environ Sci* 1986;13:3-8.
 4. Groblicki PJ. Particle Size Variation in Diesel Car Exhaust. SAE Technical Paper Series no. 790421. Warrendale: Society of Automotive Engineers, 1979.
 5. Dolan DF, Kittelson DB, Pui DY. Diesel Exhaust Particle Size Distribution Measurement Techniques. SAE Technical Paper Series no. 870254. Warrendale: Society of Automotive Engineers, 1980.
 6. NCR. Diesel Cars: Benefits, Risks, and Public Policy: Final Report of the Diesel Impacts Study Committee, Assembly of Engineering, National Research Council. Washington: National Academy Press, 1982.
 7. Williams RL. Diesel particulate emissions: Composition, concentration, and control. *Dev Toxicol Environ Sci* 1982;10:15-32.
 8. Baumgard KJ, Johnson JH. The effect of Fuel and Engine Design on Diesel Exhaust Particle Size Distributions. SAE Technical Paper Series no. 960131. Warrendale: Society of Automotive Engineers, 1996.
 9. CARB. Emission Inventory 1995. Sacramento: California Air Resources Board, 1997.
 10. Pierson WR, Brachaczek WW. Particulate matter associated with vehicles on the road II. *Aerosol Sci Tech* 1983;2:1-40.
 11. Schuetzle D, Perez JM. Factors influencing the emissions of nitrated-polynuclear aromatic hydrocarbons (nitro-PAH) from diesel engines. *J Air Pollut Control Assoc* 1983;33:751-5.
 12. Tokiwa H, Ohnishi Y. Mutagenicity and carcinogenicity of nitroarenes and their sources in the environment. *Crit Rev Toxicol* 1986;17:23-60.
 13. IPCS. Environmental Health Criteria No. 171. Diesel Fuel and Exhaust Emissions. International Program on Chemical Safety, 1996.
 14. Brightwell J, Fouillet X, Cassano-Zoppi AL, et al. Tumors of the respiratory tract in rats and hamsters following chronic inhalation of engine exhaust emissions. *J Appl Toxicol* 1989;9:23-31.
 15. Nikula KJ, Snipes MB, Barr EB, et al. Comparative pulmonary toxicities and carcinogenicities of chronically inhaled diesel exhaust and carbon black in F344 rats. *Fundam Appl Toxicol* 1995;25:80-94.
 16. Heinrich U, Fühst R, Rittinghausen S, et al. Chronic inhalation exposure of Wistar rats and two different strains of mice to diesel-engine exhaust, carbon-black, and titanium-dioxide. *Inhal Toxicol* 1995;7:533-56.
 17. IARC. Diesel and gasoline engine exhausts. In: Diesel and Gasoline Engine Exhausts and Some Nitroarenes. IARC Monographs on the Evaluation of Carcinogenic Risk of Chemicals to Humans, vol. 46. Lyon: International Agency for Research on Cancer, 1989.
 18. NTP. Report on Carcinogens Background Document for Diesel Exhaust Particulates. Research Triangle Park: National Toxicology Program, 2000.
 19. Nielsen PS, Andreassen A, Farmer PB, et al. Biomonitoring of diesel exhaust-exposed workers. DNA and hemoglobin adducts and urinary 1-hydroxypyrene as markers of exposure. *Toxicol Lett* 1996;86:27-37.
 20. Cohen AJ, Higgins MW. Health effects of diesel exhaust: Epidemiology. In: Diesel Exhaust. A Critical Analysis of Emissions, Exposure, and Health Effects. Cambridge: Health Effects Institute, 1995.
 21. Bhatia R, Lopipero P, Smith AH. Diesel exhaust exposure and lung cancer. *Epidemiology* 1998;9:84-91.
 22. Brüske-Hohlfeld I, Möhner M, Pohlabein H, et al. Occupational lung cancer risk for men in Germany: Results from a pooled case-control study. *Am J Epidemiol* 2000;151:384-95.
 23. Gustavsson P, Jakobsson R, Nyberg F, et al. Occupational exposure and lung cancer risk: A population-based case-referent study in Sweden. *Am J Epidemiol* 2000;152:32-40.
 24. Larkin EK, Smith TJ, Stayner L, et al. Diesel exhaust exposure and lung cancer: Adjustment for the effect of smoking in a retrospective cohort study. *Am J Ind Med* 2000;38:399-409.
 25. Järholm B, Silverman D. Lung cancer in heavy equipment operators and truck drivers with diesel exhaust exposure in the construction industry. *Occup Environ Med* 2003;60:516-20.
 26. Kauppinen T, Heikkilä P, Partanen T, et al. Mortality and cancer incidence of workers in Finnish road paving companies. *Am J Ind Med* 2003;43:49-57.
 27. Garshick E, Laden F, Hart JE, et al. Lung cancer in railroad workers exposed to diesel exhaust. *Environ Health Perspect* 2004;112:1539-43.
 28. Garshick E, Laden F, Hart JE, et al. Smoking imputation and lung cancer in railroad workers exposed to diesel exhaust. *Am J Ind Med* 2006;49:709-18.
 29. Garshick E, Laden F, Hart JE, et al. Lung cancer and vehicle exhaust in trucking industry workers. *Environ Health Perspect* 2008;116: 1327-32.
 30. Neumeyer-Gromen A, Razum O, Kersten N, et al. Diesel motor emissions and lung cancer mortality—results of the second follow-up of a cohort study in potash miners. *Int J Cancer* 2009;124:1900-6.
 31. Boffetta P, Silverman DT. A meta-analysis of bladder cancer

- and diesel exhaust exposure. *Epidemiology* 2001;12:125-30.
32. Boffetta P. Risk of acute myeloid leukemia after exposure to diesel exhaust: A review of the epidemiologic evidence. *J Occup Environ Med* 2004;46:1076-83.
 33. Penconek A, Arkadiusz M. Deposition of diesel exhaust particles from various fuels in a cast of human respiratory system under two breathing patterns. *J Aerosol Sci* 2013;63:48-59.
 34. Morawska L, Hofmann W, Hitchins-Loveday J, et al. Experimental study of the deposition of combustion aerosols in the human respiratory tract. *J Aerosol Sci* 2005;36:939-57.
 35. Löndahl J, Massling A, Swietlicki E, et al. Experimentally determined human respiratory tract deposition of airborne particles at a busy street. *Environ Sci Technol* 2009;43:4659-64.
 36. Rissler J, Swietlicki E, Bengtsson A, et al. Experimental determination of deposition of diesel exhaust particles in the human respiratory tract. *J Aerosol Sci* 2012;48:18-33.
 37. Hofmann W, Sturm R, Winkler-Heil R, et al. Stochastic model of ultrafine particle deposition and clearance in the human respiratory tract. *Radiat Prot Dosimetry* 2003;105:77-80.
 38. Sturm R. Deposition and cellular interaction of cancer-inducing particles in the human respiratory tract: Theoretical approaches and experimental data. *Thoracic Cancer* 2010;4:141-52.
 39. Sturm R. Theoretical and experimental approaches to the deposition and clearance of ultrafine carcinogens in the human respiratory tract. *Thoracic Cancer* 2011;2:61-8.
 40. Sturm R. Theoretical models of carcinogenic particle deposition and clearance in children's lungs. *J Thorac Dis* 2012;4:368-76.
 41. Sturm R. Theoretical deposition of carcinogenic particle aggregates in the upper respiratory tract. *Ann Transl Med* 2013;1:25.
 42. Sturm R. Total deposition of ultrafine particles in the lungs of healthy men and women: experimental and theoretical results. *Ann Transl Med* 2016;4:234.
 43. Sturm R. Inhaled nanoparticles. *Phys Today* 2016;69:70-1.
 44. Sturm R. Deposition of ultrafine particles with various shapes in the human alveoli – a model approach. *Comput Mat Biol* 2016;5:4.
 45. Koblinger L, Hofmann W. Analysis of human lung morphometric data for stochastic aerosol deposition calculations. *Phys Med Biol* 1985;30:541-56.
 46. Koblinger L, Hofmann W. Monte Carlo modeling of aerosol deposition in human lungs. Part I: simulation of particle transport in a stochastic lung structure. *J Aerosol Sci* 1990;21:661-74.
 47. Sturm R, Hofmann W. A computer program for the simulation of fiber deposition in the human respiratory tract. *Comput Biol Med* 2006;36:1252-67.
 48. Sturm R. Theoretical approach to the hit probability of lung-cancer-sensitive epithelial cells by mineral fibers with various aspect ratios. *Thoracic Cancer* 2010;3:116-25.
 49. Sturm R. Theoretical deposition of nanotubes in the respiratory tract of children and adults. *Ann Transl Med* 2014;2:6.
 50. Sturm R. Nanotubes in the respiratory tract - Deposition modeling. *Z Med Phys* 2015;25:135-45.
 51. Sturm R. Spatial visualization of nanoparticle deposition in the human respiratory tract. *Ann Transl Med* 2015;3:326.
 52. Sturm R. A stochastic model of carbon nanotube deposition in the airways and alveoli of the human respiratory tract. *Inhal Toxicol* 2016;28:49-60.
 53. Sturm R. Computer-aided generation and lung deposition modeling of nano-scale particle aggregates. *Inhal Toxicol* 2017. [Epub ahead of print].
 54. Kasper G. Dynamics and measurement of smokes. I Size characterization of non-spherical particles. *Aerosol Sci Technol* 1982;1:187-99.
 55. Sturm R. Theoretical models for dynamic shape factors and lung deposition of small particle aggregates originating from combustion processes. *Z Med Phys* 2010;20:226-34.
 56. Sturm R, Hofmann W. A theoretical approach to the deposition and clearance of fibers with variable size in the human respiratory tract. *J Hazard Mater* 2009;170:210-8.
 57. Sturm R. Modeling the deposition of bioaerosols with variable size and shape in the human respiratory tract - A review. *J Adv Res* 2012;3:295-304.
 58. International Commission on Radiological Protection (ICRP). *Human Respiratory Tract Model for Radiological Protection*, Publication 66. Oxford: Pergamon Press, 1994.
 59. Sturm R, Hofmann W, Scheuch G, et al. Particle clearance in human bronchial airways: Comparison of stochastic model predictions with experimental data. *Ann Occup Hyg* 2002;46:329-39.
 60. Sturm R, Hofmann W. Mechanistic interpretation of the slow bronchial clearance phase. *Radiat Prot Dosimetry* 2003;105:101-4.
 61. Hofmann W, Sturm R. Stochastic model of particle clearance in the human bronchial airways. *J Aerosol Med* 2004;17:73-89.
 62. Sturm R, Hofmann W. A multi-compartment model for slow bronchial clearance of insoluble particles—extension

- of the ICRP human respiratory tract models. *Radiat Prot Dosimetry* 2006;118:384-94.
63. Sturm R. A computer model for the clearance of insoluble particles from the tracheobronchial tree of the human lung. *Comput Biol Med* 2007;37:680-90.
64. Sturm R. A computer model for the simulation of fiber-cell interaction in the alveolar region of the respiratory tract. *Comput Biol Med* 2011;41:565-73.
65. Sturm R. A three-dimensional model of tracheobronchial particle distribution during mucociliary clearance in the human respiratory tract. *Z Med Phys* 2013;23:111-9.

doi: 10.21037/jphe.2017.06.07

Cite this article as: Sturm R. Deposition of diesel exhaust particles in the human lungs: theoretical simulations and experimental data. *J Public Health Emerg* 2017;1:70.